Sequential signals toward podosome formation in NIH-src cells

Tsukasa Oikawa,[1] Toshiki Itoh,[2] and Tadaomi Takenawa[1]

[1]Division of Lipid Biochemistry and [2]Division of Membrane Biology, Department of Biochemistry and Molecular Biology, Kobe University Graduate School of Medicine, 7-5-1 Kusunoki-cho, Chuo-ku, Kobe, Hyogo 650-0017, Japan

Podosomes (also termed invadopodia in cancer cells) are actin-rich adhesion structures with matrix degradation activity that develop in various cell types. Despite their significant physiological importance, the molecular mechanism of podosome formation is largely unknown. In this study, we investigated the molecular mechanisms of podosome formation. The expression of various phosphoinositide-binding domains revealed that the podosomes in Src-transformed NIH3T3 (NIH-src) cells are enriched with PtdIns(3,4)P2, suggesting an important role of this phosphoinositide in podosome formation. Live-cell imaging analysis revealed that Src-expression stimulated podosome formation at focal adhesions of NIH3T3 cells after PtdIns(3,4)P2 accumulation. The adaptor protein Tks5/FISH, which is essential for podosome formation, was found to form a complex with Grb2 at adhesion sites in an Src-dependent manner. Further, it was found that N-WASP bound all SH3 domains of Tks5/FISH, which facilitated circular podosome formation. These results indicate that augmentation of the N-WASP–Arp2/3 signal was accomplished on the platform of Tks5/FISH-Grb2 complex at focal adhesions, which is stabilized by PtdIns(3,4)P2.

Introduction

Podosomes/invadopodia are cellular appendages that are formed on the ventral surface of the plasma membrane perpendicular to and in contact with the extracellular matrix (ECM). They appear to be involved in a wide range of physiological and pathological aspects such as sealing-ring formation in osteoclasts (Destaing et al., 2003; Jurdic et al., 2006), transcellular diapedesis of leukocytes (Carman et al., 2007), and invasion of cancer cells into the ECM (Yamaguchi et al., 2006).

They comprise dot-shaped, F-actin–rich contact regions that appear as small (diameter of 1–2 µm and depth of 200–400 nm) plasma membrane extensions when observed under an electron microscope; they assemble at an early stage during cell adhesion to a substrate. They are enriched with adhesion molecules, actin-modulating proteins, tyrosine kinases, matrix proteases, and tyrosine-phosphorylated proteins (David-Pfeuty and Singer, 1980; Tarone et al., 1985; Marchisio et al., 1988; Buccione et al., 2004; Gimona, 2008). Among them, the Arp2/3 complex and its activators Wiskott-Aldrich syndrome protein (WASP) or N-WASP in nonhematopoietic cells are the primary machinery for the assembly of F-actin columns in various cell types (Mizutani et al., 2002; Yamaguchi et al., 2005; Olivier et al., 2006). Upstream regulators of N-WASP including Cdc42, Nck1, and WIP, have also been proved to be essential for EGF-induced invadopodia formation in mammary carcinoma cells (Yamaguchi et al., 2005), thereby confirming the importance of this molecule. However, the precise pathways regarding the spatio-temporal orchestration leading to WASP/N-WASP–induced actin polymerization is largely unknown.

Many studies have revealed that the hyperactivity of c-Src is responsible for several human malignancies, especially colon and breast carcinoma (Yeatman, 2004; Alvarez et al., 2006). c-Src is also essential for osteoclast activity in vivo, because Src knockout mice suffer from severe osteopetrosis caused by deficient osteoclast activity (Soriano et al., 1991). Although c-Src increases cell proliferation, its primary role is considered to be the regulation of cell adhesion, invasion, and motility. Additional evidence that Src-transformed cells bear podosomes/invadopodia has lead to the belief that c-Src plays a role as a major generator of this structure. Tks5/FISH was first identified as an Src substrate with one phox homology (PX) domain and five Src homology 3 (SH3) domains (Lock et al., 1998). Later, Tks5/FISH was found to be localized at the podosomes of Src-transformed cells (Abram et al., 2003). Further, Tks5/FISH was proved to be highly expressed in malignant carcinoma tissues

Correspondence to Tadaomi Takenawa: takenawa@med.kobe-u.ac.jp

Abbreviations used in this paper: FA, focal adhesion; FAK, focal adhesion kinase; PH, pleckstrin homology; PX, phox homology; SH3, Src homology 3; TIRF, total internal reflection fluorescence; WASP, Wiskott-Aldrich syndrome protein.

The online version of this paper contains supplemental material.

J. Cell Biol. Vol. 182 No. 1 157–169
www.jcb.org/cgi/doi/10.1083/jcb.200801042

and has been shown to play a pivotal role in podosome formation and ECM degradation (Seals et al., 2005). Although the importance of the PX domain and several binding proteins of the SH3 domains are suggested in all the research on Tks5/FISH, a comprehensive understanding regarding its role in podosome formation is yet to be achieved.

Substantial evidence has recently revealed that phosphoinositides bind to and regulate a number of cytoskeletal proteins (Takenawa and Itoh, 2001). Among them, PtdIns(3)-kinase products such as PtdIns(3,4,5)P3 and PtdIns(3,4)P2, which are present in negligible amounts under resting conditions, are formed at the plasma membrane in response to extracellular stimuli. Further, these locally produced PtdIns(3,4,5)P3 and PtdIns(3,4)P2 recruit cytosolic proteins to the plasma membrane. Consequently, proteins that specifically bind these phosphoinositides play important roles in extracellular signal-dependent cytoskeletal remodelling, membrane trafficking, cell proliferation, and apoptosis (Itoh and Takenawa, 2004; Takenawa and Itoh, 2006). The proteins within podosomes are presumably influenced by phosphoinositides. For example, PtdIns(3,4,5)P3 is able to modulate the functions of small GTPases of the Rho family, such as Rho, Rac, and Cdc42; these proteins are believed to be involved in podosome formation (Chellaiah, 2006). This modulation occurs via the action of guanine nucleotide exchange factors (GEFs) such as Tiam1, Vav1, and SWAP70 on these proteins; all these factors possess pleckstrin homology (PH) domains via which they interact with PtdIns(3,4,5)P3. However, it remains unclear how these lipids participate in podosome formation.

Here, we demonstrate that PtdIns(3,4)P2 and Grb2 at focal adhesions cooperatively recruit the adaptor protein Tks5/FISH before actin polymerization at podosomes. Further, N-WASP was found to bind Tks5/FISH depending on its SH3 domains, and it contributes to circular podosome formation. Based on these observations, we propose a novel model for podosome formation, particularly the initiation phase.

Results

PtdIns(3,4)P2 plays an important role in podosome formation in NIH-src cells

We first examined the involvement of PtdIns(3)-kinase in podosome formation because of its importance in cell migration and in establishing cell polarity. As with PP2 (an Src kinase inhibitor), treatment with LY294002 (a PtdIns(3)-kinase inhibitor) resulted in the disappearance of podosomes, indicating the involvement of PtdIns(3)-kinase activity in podosome formation (Fig. S1 A, available at http://www.jcb.org/cgi/content/full/jcb.200801042/DC1). This ability to suppress podosome formation correlated with the inhibition of invasion (Fig. S1, B and C), and it supports the role of podosomes in ECM invasion. Next, we used various phosphoinositide-binding domains to detect the localization of intracellular phosphoinositides (Furutani et al., 2006). The FYVE domain of Hrs binds specifically to PtdIns(3)P, and it was distributed at endosome-like dots in NIH-src cells (Fig. 1 A). The PH domains of Fapp1 and PLCδ1 bound specifically to PtdIns(4)P and PtdIns(4,5)P2, respectively, and they were localized at the Golgi apparatus and plasma membrane (Fig. 1 A). It is noteworthy that PtdIns(3,4)P2, which was specifically detected by the PH domain of Tapp1 (hereafter referred to as Tapp1PH), was strongly concentrated at the podosomes (Fig. 1 A). On the other hand, PtdIns(3,4,5)P3, which was detected by the PH domain of Grp1 (Grp1PH), was localized at the podosomes, although it was also present at other areas, including at ruffles and intracellular vesicles (Fig. 1 A). Expectedly, the localization of the PH domain of Akt, which recognizes both PtdIns(3,4)P2 and PtdIns(3,4,5)P3, was like a superimposed image of Tapp1PH and Grp1PH (Fig. 1 A). Tapp1PH, when weakly expressed, favored localization at podosomes; however, its overexpression (including weak and strong expression) tended to suppress podosome formation. Approximately 20% suppression was observed when Tapp1PH was expressed as compared with when its lipid-binding inactive form (Tapp1PH R212L) was expressed (Fig. 1 B). Compared with its mutants (AktPH R25A and AktPH K14A), AktPH also suppressed podosome formation by ∼35% (Fig. 1 B). These results indicate that the plasma membrane of podosomes is enriched with PtdIns(3,4)P2 and that the interference of binding between this phosphoinositide and its targets inhibits podosome formation. However, because the inhibitory effect of Tapp1PH expression was not so efficient, there is a possibility that other mechanisms are also involved in the formation of podosomes.

Constitutive active Src induces PtdIns(3,4)P2 production at focal adhesions, which triggers podosome formation

Because Tks5/FISH—a recently identified adaptor molecule essential for podosome formation (Seals et al., 2005)—contains a PX domain in its N terminus (Fig. S2 A, available at http://www.jcb.org/cgi/content/full/jcb.200801042/DC1), we expected this domain to be one of the targets of phosphoinositides at podosomes. Actually, the PX domain of Tks5/FISH is reported to bind with a high affinity to PtdIns(3)P and PtdIns(3,4)P2 (Abram et al., 2003). In support of this, the wild type of the PX domain accumulated on both endosome-like dots and podosomes, whereas its lipid-binding inactive form (PX R42A/R93A) did not accumulate on them (Fig. S2, B–D). Further, the expression of the PX domain tended to suppress podosome formation to ∼20%, which is significant when compared with the PX R42A/R93A mutant or the delta-PX mutant of Tks5/FISH (Fig. S2 E). This suggests that PtdIns(3,4)P2 plays an important role in podosome formation by interacting with Tks5/FISH via its PX domain. More importantly, the PX R42A/R93A mutant also significantly suppressed podosome formation as compared with the delta-PX mutant (Fig. S2 E); this ascribes the inhibitory effect by the PX domain to additional mechanisms involving lipid interaction, which would explain the relatively effective suppression by the PX domain as compared with that by Tapp1PH or AktPH.

To determine whether the accumulation of PtdIns(3,4)P2 at podosomes is a result or cause of podosome formation, we examined the localization of this phosphoinositide in NIH-src cells with reduced Tks5/FISH expression. Reduced Tks5/FISH

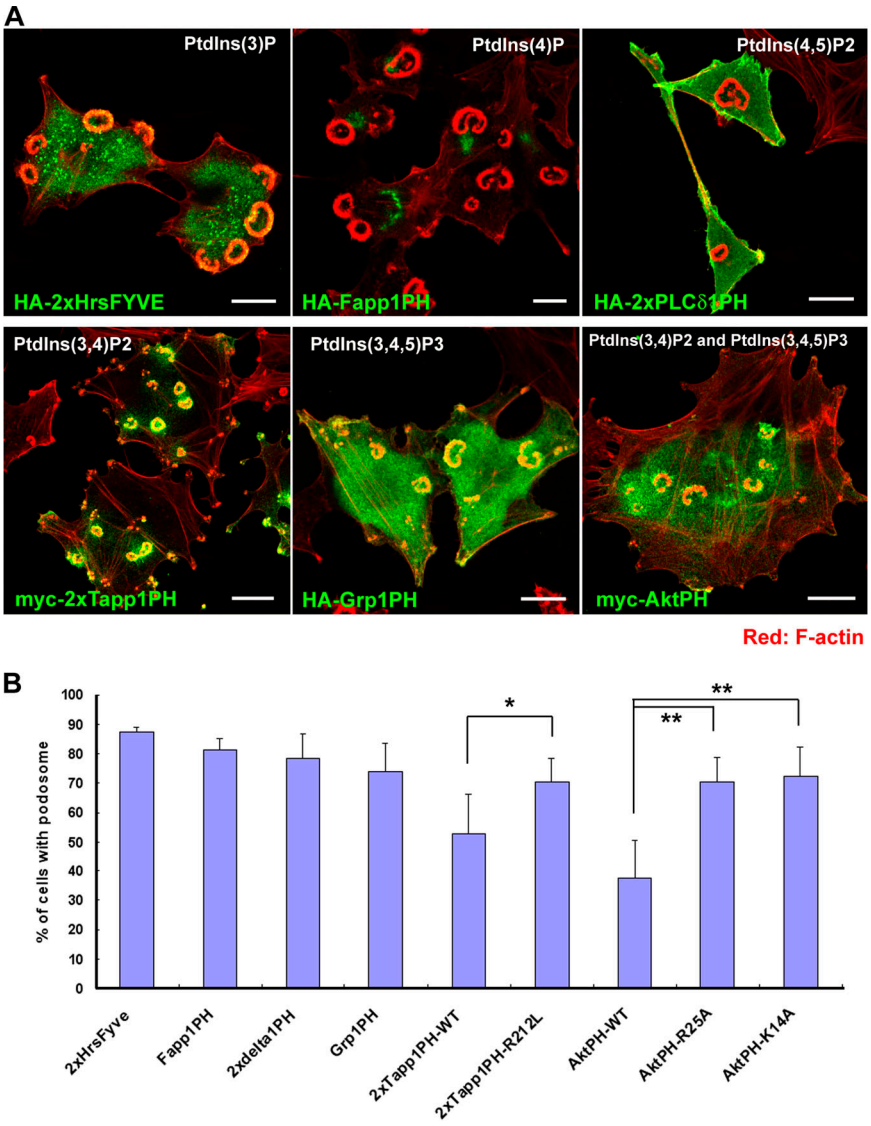

Figure 1. **The plasma membrane at the podosomes in NIH-src cells is enriched with PtdIns(3,4)P2.** (A) Localization of phosphoinositide-binding domains in NIH-src cells. PtdIns(3)P, PtdIns(4)P, PtdIns(4,5)P2, PtdIns(3,4)P2, and PtdIns(3,4,5)P3 were localized by the FYVE domain of Hrs and the PH domains of Fapp1, PLCδ1, Tapp1, Grp1, and Akt, respectively. In the figure, 2× indicates two domains linked in tandem. The binding specificity of the constructs for each domain has been described previously (Furutani et al., 2006). The cells were stained with rhodamine-phalloidin (red) to visualize F-actin with anti-HA or anti-myc antibody (green). Bars, 20 µm. (B) Quantification of podosomes in NIH-src cells expressing lipid-binding domains (regardless of its expression amount). Error bars represent the standard deviations of three independent measurements. *, $P < 0.04$; **, $P < 0.02$ by Student's *t* test compared with each mutant (Tapp1PH and AktPH). A minimum of 50 cells were counted for each determination.

expression in NIH-src cells resulted in the disappearance of podosomes (Fig. 2 A and Fig. S2 F) and invasion (Fig. S2 G), whereas that in the control (NIH-ctr) cells caused imperceptible morphological changes (Fig. S2, H and I). Tapp1PH in NIH-ctr cells localized at ruffling areas and the suppression of Tks5/FISH expression in these cells had virtually no effect on its distribution (Fig. S2 I, arrowheads). Notably, the polarized distribution of Tapp1PH persisted even when the Tks5/FISH expression was suppressed in NIH-src cells (Fig. 2 A), suggesting that the polarization of the plasma membrane is achieved independent of Tks5/FISH and podosome formation; i.e., this might be a trigger for podosome formation that precedes Tks5/FISH recruitment. By staining with an antibody against focal adhesion kinase (FAK), we confirmed that the polarization of the membrane is achieved at adhesion sites of the NIH-src cells (hereafter referred to as focal adhesion [FA]-related adhesions) (Fig. 2 B, arrowheads). To confirm that normal focal adhesions (FAs) are precursors of podosomes, we used time-lapse observation of NIH3T3 cells expressing GFP-vinculin and RFP-2×Tapp1PH. We introduced pcDNA-SrcY530F plasmid 3 h before starting the observation, and found that some cells began to bear podosomes in 1–2 h. At the transition state, polarization of 2×Tapp1PH was observed in the vicinity of newly formed vinculin-positive FAs (Fig. 2 C, arrowheads), resulting in rearrangement of vinculin (Fig. 2 C, arrows) and ring-shaped podosomes (Fig. 2 C). On the other hand, NIH-src cells also began to assemble podosomes at FA-related adhesions when spreading (Fig. S3, available at http://www.jcb.org/cgi/content/full/jcb.200801042/DC1), supporting the notion that podosomes are initiated at FAs. These results indicate that the constitutive activation of Src alters the phosphoinositides at the proximal membrane of the FAs, and that the resulting FA-related adhesions are essential for the subsequent actin polymerization at podosomes.

Grb2 aids Tks5/FISH recruitment to focal adhesions in an Src-dependent manner

To examine the idea that Tks5/FISH recruitment to FAs is responsible for podosome formation, we used an immunoprecipitation assay with antibodies against FA molecules. As the adaptor

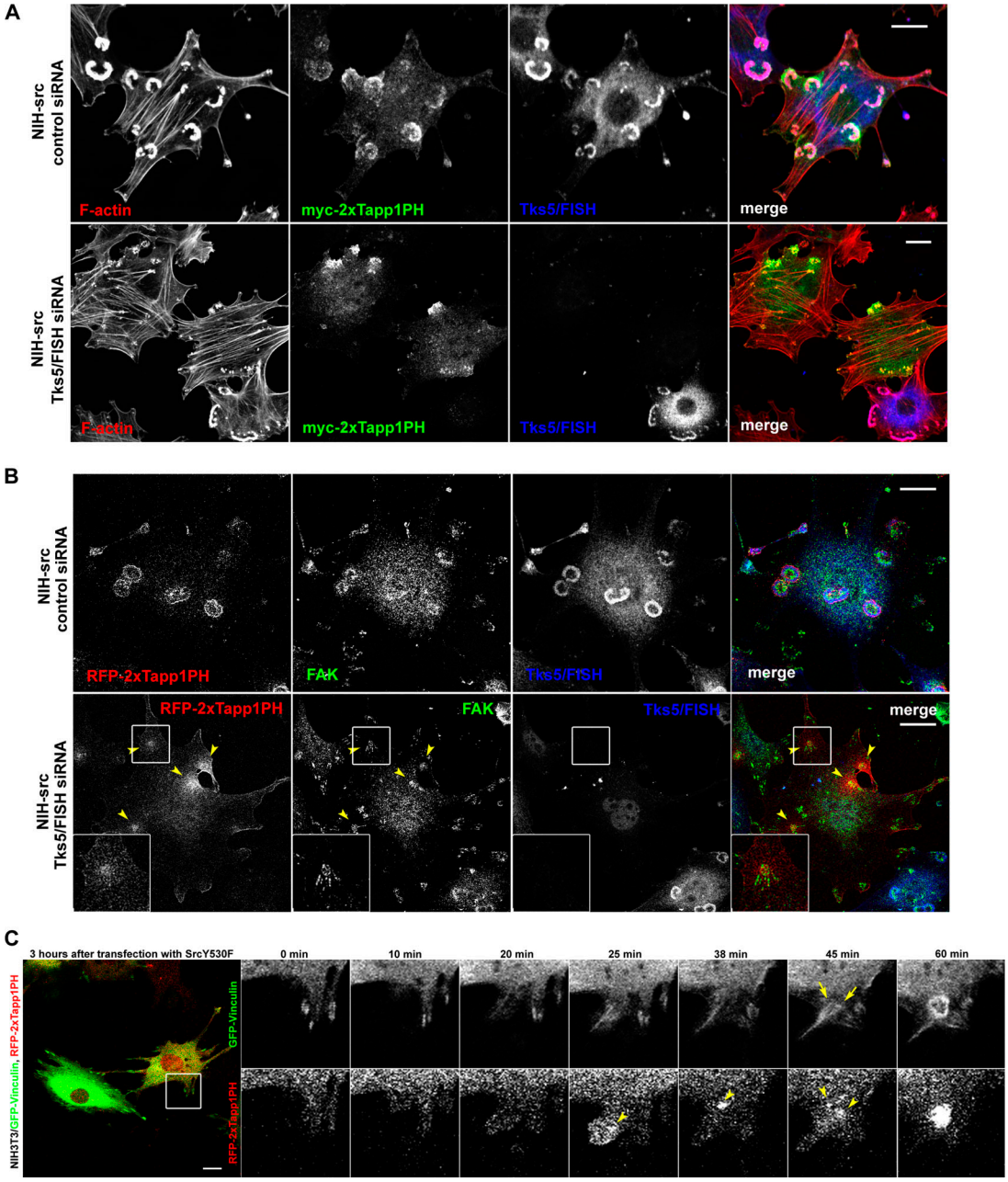

Figure 2. **Podosomes assemble at the proximal part of focal adhesions followed by PtdIns(3,4)P2 accumulation.** (A) NIH-src cells with reduced Tks5/FISH expression expressing myc-tagged Tapp1PH were stained with rhodamine-phalloidin (red) to visualize F-actin with anti-myc antibody (green) and anti-Tks5/FISH antibody (blue). (B) NIH-src cells with reduced Tks5/FISH expression expressing RFP-2×Tapp1PH were stained with anti-FAK antibody (green) and with anti-Tks5/FISH antibody (blue). Arrowheads indicate the polarization of the plasma membrane at FA-related adhesions. The regions outlined by boxes are examples of FA-related adhesions magnified twofold. Bars, 20 µm. (C) NIH3T3 cells were transfected with GFP-vinculin and RFP-2×Tapp1PH on the previous day of transfection with pcDNA-SrcY530F plasmid. The cells were cultured in fresh medium 3 h after the transfection and the observations were started. The region outlined by a box is an example of newly formed FA, which was associated with a podosome (magnified and shown with elapsed time points). Arrowheads indicate the accumulation of 2×Tapp1PH and arrows indicate a developing podosome. Bars, 20 µm.

proteins Nck, Crk, and Grb2 have been reported to play important roles in adhesion-mediated cytoskeletal changes through interaction with adhesion molecules such as FAK or p130Cas, we examined their involvement in podosome formation and binding ability to Tks5/FISH. When expressed in NIH-src cells, the SH2 domains of Grb2 and Crk significantly suppressed podosome formation, whereas the SH2 domain of Nck did not (Fig. 3 A). Further, reduced expression of Grb2 and Crk, but not Nck1 (Fig. S4, A–C; available at http://www.jcb.org/cgi/content/full/jcb.200801042/DC1) resulted in the suppression of podosomes, indicating that Grb2 and Crk play important roles in podosome formation (Fig. 3 A). On the other hand, invasion activity of NIH-src cells with reduced Nck1 expression did not correlate with podosome formation activity; they showed significant suppression of invasion as did the cells with reduced expression of Grb2 and Crk (Fig. S4 D). These results suggest that Nck1 is

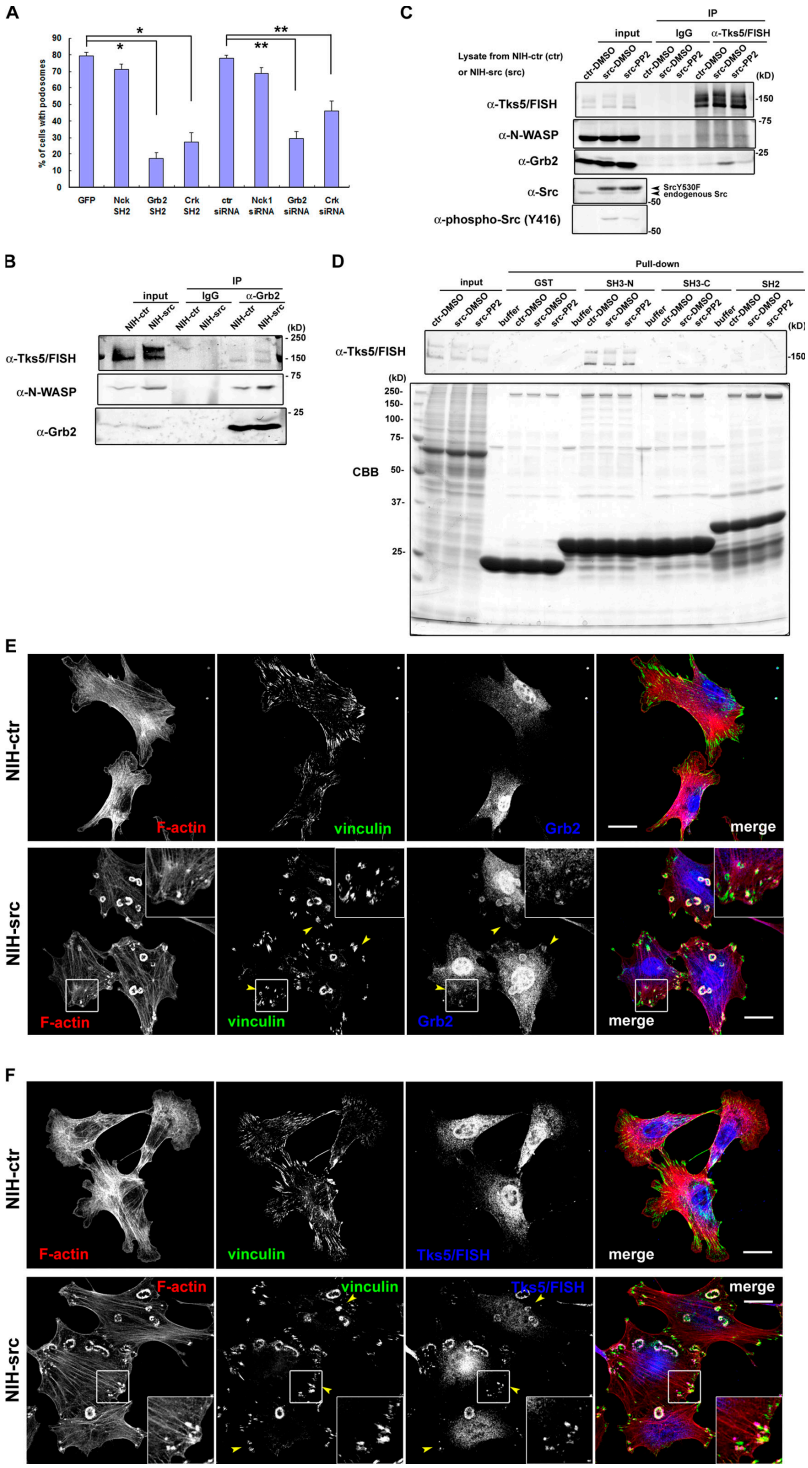

Figure 3. **Tks5/FISH binds with Grb2 in an Src-dependent manner.** (A) Myc-tagged SH2 domain of Nck, Grb2, or Crk was expressed in NIH-src cells, and the cells with podosomes were counted. For RNAi experiments, the NIH-src cells were transfected with each siRNA. The percentage of transfected cells that developed podosomes was calculated. Error bars represent the standard deviation of three different measurements. *, $P < 0.002$ by Student's *t* test compared with GFP. **, $P < 0.001$ by Student's *t* test compared with control siRNA. A minimum of 50 cells were counted for each determination. (B and C) Immunoprecipitations with anti-Grb2 (B) or anti-Tks5/FISH (C) were performed as described in Materials and methods. Western blot was performed by cropping the original membrane according to the molecular weight of Tks5/FISH, N-WASP, and Grb2, respectively, to detect them simultaneously. The bound proteins were analyzed by using anti-Tks5/FISH, anti-N-WASP, or anti-Grb2 antibody. (D) NIH-ctr or NIH-src cell lysates were mixed with the GST-SH3 or GST-SH2 domains of Grb2 immobilized on beads; the bound proteins were resolved by SDS-PAGE, and Tks5/FISH was detected by using anti-Tks5/FISH antibody. (E and F) Grb2 (E) or Tks5/FISH (F) (blue) in NIH-ctr cells and NIH-src cells was stained with anti-Grb2 (rabbit polyclonal) or anti-Tks5/FISH, respectively. They were co-stained with rhodamine-phalloidin (red) and anti-vinculin (green) as an adhesion marker. Arrowheads indicate the FA-related adhesions of NIH-src cells where Grb2 or Tks5/FISH accumulated. The regions outlined by boxes are examples of FA-related adhesions magnified twofold. Bars, 20 μm.

involved in matrix invasion via other mechanisms than podosome formation. Then, we performed an immunoprecipitation assay by using anti-Grb2 or anti-Crk antibody, and we found that only Grb2 precipitated Tks5/FISH in an Src-dependent manner (Fig. 3 B, N-WASP as a positive control; discussed in Fig. 6). This interaction was confirmed by immunoprecipitation with an anti-Tks5/FISH antibody; Grb2 was coimmunoprecipitated in an Src-dependent manner (Fig. 3 C), whereas Crk was not (unpublished data; the involvement of Crk is presented in the Discussion section). This interaction is thought to be mediated by the poly-proline sequences of Tks5/FISH (sporadically found between the SH3 domains) with the N-terminal SH3 domain of Grb2 (Fig. 3 D). To visualize the Src-dependent translocation of Grb2 or Tks5/FISH, we observed endogenous Grb2 or Tks5/FISH together with vinculin in NIH-ctr and NIH-src cells. In NIH-ctr cells, neither Grb2 (Fig. 3 E, top panels) nor Tks5/FISH (Fig. 3 F, top panels) was concentrated at vinculin-positive adhesion sites. In contrast, both were translocated

not only to podosomes but also to vinculin-positive FA-related adhesions in NIH-src cells (Fig. 3, E and F; bottom panels, arrowheads). Grb2 was still observed at PtdIns(3,4)P2-enriched FA-related adhesions of NIH-src cells with reduced Tks5/FISH expression, suggesting the translocation was independent of Tks5/FISH (Fig. S4 E). However, compared with Tks5/FISH, Grb2 showed weaker concentration at podosomes; this would explain the small amount of Tks5/FISH in anti-Grb2 immunoprecipitates (Fig. 3 B), while the substantial amount of Grb2 was detected in anti-Tks5/FISH immunoprecipitates (Fig. 3 C). Collectively, these results indicate that the constitutive activation of c-Src facilitates a complex formation of Grb2-Tks5/FISH in parallel with PtdIns(3,4)P2 generation at FA-related adhesions, which is a hallmark of podosomes-to-be. To localize correctly, Tks5/FISH must be recruited to podosomes not only through PtdIns(3,4)P2 but also through protein complex formation.

Grb2 and Tks5/FISH translocate to focal adhesions in an Src-dependent and F-actin–independent manner

To clearly elucidate the molecular events that occur before actin polymerization, the Src-dependent and F-actin–independent translocation of these molecules in connection with PtdIns(3,4)P2 generation was observed. NIH-src cells expressing these molecules were treated with PP2 and latrunculin B followed by only latrunculin B treatment. This treatment enabled the recovery of Src activity in 40 min (Fig. 4, A and B; phospho-Src [Y416] column) with F-actin kept depolymerized. As Src recovered its activity within 40 min after PP2 wash out, PtdIns(3,4)P2 detected by 2×Tapp1PH or Grb2 was observed at phospho-Src (Y416)-positive FA-related adhesions (Fig. 4, A and B; bottom panels). Tks5/FISH, on the other hand, was found to have merged with these sites (Fig. 4, A and B; bottom panels, arrowheads). These results indicate that constitutive Src activation leads to PtdIns(3,4)P2 generation and Grb2 recruitment to FA-related adhesions, where Tks5/FISH is also recruited independent of actin polymerization. Thus, the puncta of Grb2 and Tks5/FISH observed in Fig. 4 B are considered podosome precursors that would develop into podosomes.

Live-cell imaging analysis of podosome-precursor formation

To confirm the molecular dynamics of podosome-precursor formation at the proximal part of the adhesion sites, the localization of PtdIns(3,4)P2, Grb2, and Tks5/FISH was detected in live cells by using total internal reflection fluorescence (TIRF) microscopy. First, we observed NIH-src cells expressing either RFP-2×Tapp1PH or RFP-Grb2 together with GFP-Tks5/FISH. For the same purpose as the previous section, the cells expressing these molecules were treated with PP2 and latrunculin B followed by only latrunculin B treatment. RFP-2×Tapp1PH began to distribute in a polarized way right after the PP2 wash out, followed by the gradual accumulation of GFP-Tks5/FISH (Fig. 5 A, arrowheads). The relative pixel intensity of the region of interest (ROI, RFP/GFP) tended to show a sharp increase due to early PtdIns(3,4)P2 accumulation, and it then converged to a constant value when Tks5/FISH was recruited to this region (Fig. 5 A, chart). Grb2 accumulation appeared to precede Tks5/FISH recruitment, and they were observed to move synchronously to form podosome-shaped accumulations (Fig. 5 B, arrowheads). Next, we examined whether the FA-related adhesions with PtdIns(3,4)P2, observed in Figs. 4 A and 5 A, would develop into a podosome. NIH-src cells expressing RFP-2×Tapp1PH and YFP-actin were pretreated with PP2 and latrunculin B to block podosome formation, and then the drugs were completely washed out. As expected, FA-related adhesion with persistent PtdIns(3,4)P2 production resulted in circular podosome formation (Fig. 5 C). The relative pixel intensity of the ROI (RFP/YFP) tended to show a similarity with that of Fig. 5 A, indicating that Tks5/FISH recruitment correlates with actin polymerization. These results suggest that the Src-driven formation of the Tks5/FISH-Grb2 complex (podosome precursor) occurs on the site of action; i.e., PtdIns(3,4)P2-enriched FA-related adhesions before actin polymerization, and then circular podosomes develop on this site.

Tks5/FISH enhances N-WASP–dependent actin polymerization

Accumulated evidence has demonstrated that the N-WASP-Arp2/3 pathway is indispensable for actin polymerization in podosomes/invadopodia of many cell types (Linder et al., 1999, 2000; Mizutani et al., 2002; Yamaguchi et al., 2005). We examined whether Tks5/FISH mediates N-WASP–dependent actin polymerization by interacting with it. Immunoprecipitation of Tks5/FISH identified N-WASP as a binding partner, although the binding was constitutive (Fig. 3 C). To identify other molecules involved in podosome-precursor formation, we used a pull-down assay using each domain of Tks5/FISH (Fig. S2 A). To this end, GST-tagged PX or SH3 domains of Tks5/FISH were immobilized on glutathione-sepharose beads, incubated with NIH-src cell lysates, and then washed intensively. The proteins that bound to the PX domain or any of the SH3 domains of Tks5/FISH were resolved by SDS-PAGE and then subjected to mass spectrometry (Fig. 6 A, left panel). The following proteins were identified with no ambiguity: dynamin 2 (bound to SH3A and E: band a); N-WASP (bound to SH3A, B, C, D, and E: band b); WIP (bound to SH3C and E); tubulin (bound to SH3C); zyxin (bound to SH3C and E); nogo-B (bound to SH3E); and actin (bound to SH3E). The interaction of N-WASP and dynamin with the SH3 domains of Tks5/FISH was validated by performing Western blotting using anti-N-WASP and anti-dynamin antibodies, respectively (Fig. 6 A, right). However, we could not detect dynamin in Tks5/FISH immunoprecipitates (unpublished data). Because all the SH3 domains of Tks5/FISH can bind to N-WASP, we expected Tks5/FISH to assemble a large amount of N-WASP at FA-related adhesions, leading to strong actin polymerization by the Arp2/3 complex. Actually, Grb2 precipitated more N-WASP from the cell lysate of NIH-src cells than from that of NIH-ctr cells (Fig. 3 B). Three truncated constructs containing different number of the SH3 domains were synthesized to test whether Tks5/FISH binding to N-WASP depends on these domains (Fig. 6 B). The cell lysates of the NIH3T3 cells expressing GFP-tagged-Tks5/FISH constructs were immunoprecipitated using anti-GFP antibody,

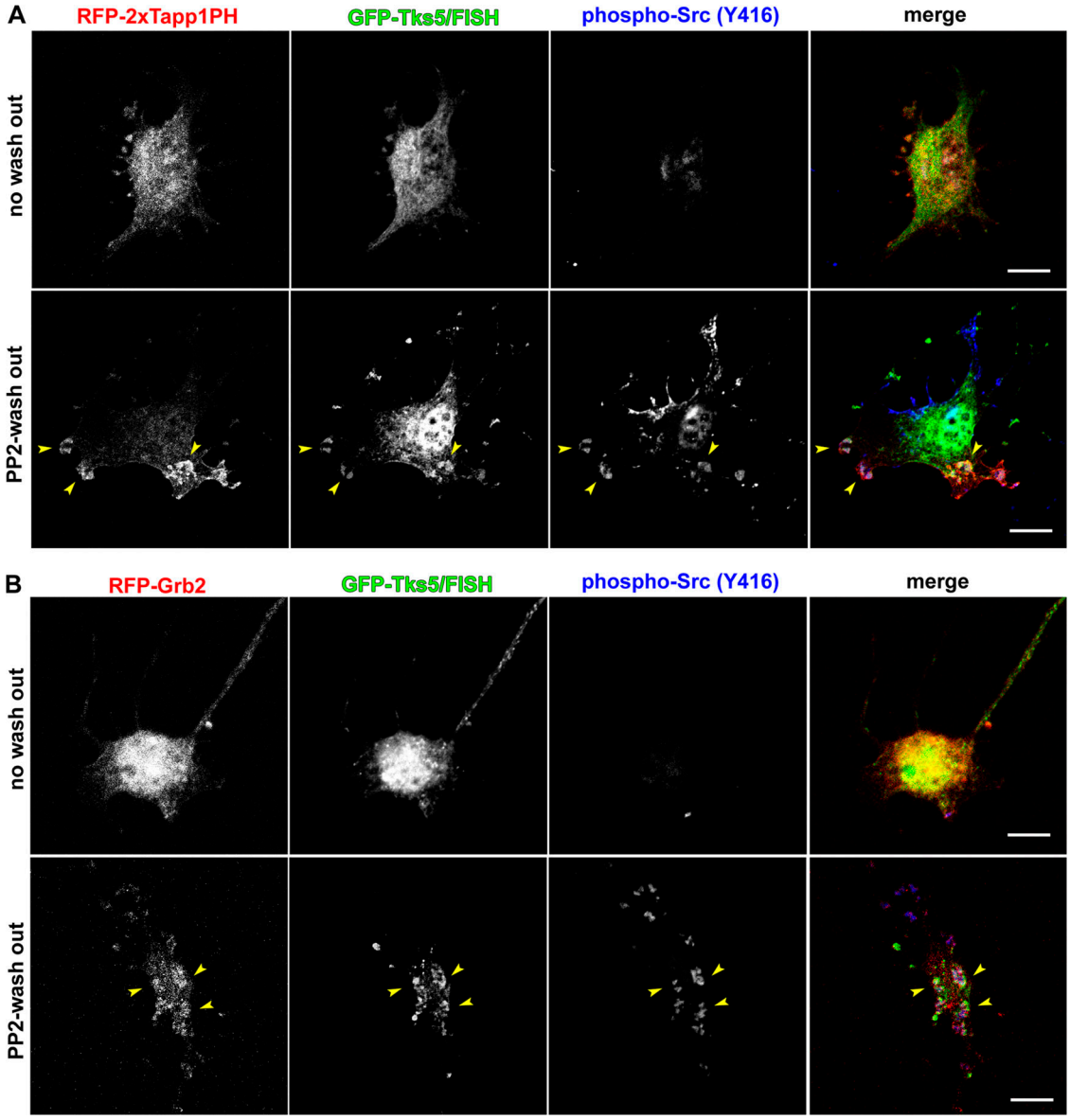

Figure 4. **Grb2 and Tks5/FISH translocate to FA-related adhesions depending on Src kinase activity.** (A and B) NIH-src cells transfected with either RFP-2×Tapp1PH (A) or RFP-Grb2 (B) (red) together with GFP-Tks5/FISH (green) were cultured in fresh medium with latrunculin B (0.5 µg/ml), after the treatment with PP2 (10 µM) and latrunculin B (0.5 µg/ml) for 30 min (PP2-wash out row). The cells were then fixed at 40 min and stained with anti-phospho-Src (Y416) (blue). Arrowheads indicate merged areas of the expressed proteins and phospho-Src. Bars, 20 µm.

and the bound protein was detected by Western blotting using anti-N-WASP antibody (Fig. 6 C). The amount of N-WASP coprecipitated increased with the number of SH3 domains, indicating that five SH3 domains of Tks5/FISH can bind to N-WASP more efficiently than one or three SH3 domains. As the expression of the poly-proline sequence of N-WASP (N-WASP PP) significantly suppressed podosome formation (Fig. 6 D), this binding activity appears to be related to the ability of the cells to develop podosomes; the recruitment of a large amount of N-WASP to FA-related adhesions is required for mature podosome formation. When the three constructs were expressed in NIH-src cells having reduced Tks5/FISH expression, the cells recovered podosome formation depending on the SH3 domains they expressed (Fig. 6, E and F). Interestingly, some cells expressing PX-SH3A or PX-SH3C exhibited aberrant podosomes that were either fragmented or not sufficiently thick (Fig. 6 E, arrowheads). These aberrant podosomes resemble those observed in v-Src^{+}/N-WASP$^{-/-}$ fibroblasts expressing a mutant N-WASP that cannot interact with barbed ends (Co et al., 2007). Thus, they are considered to originate from the attenuation of N-WASP recruitment to the sites of action.

Delta-VCA mutant of N-WASP forms a ring-shaped podosome-like structure

Because the verproline-homology (V) and cofilin-homology and acidic (CA) regions of the WASP family proteins contribute to rapid actin polymerization by binding G-actin and the Arp2/3 complex, respectively, mutants that lack the VCA region (delta-VCA) serve as dominant-negative forms of N-WASP function (Fig. S5, A and B; available at http://www.jcb.org/cgi/content/

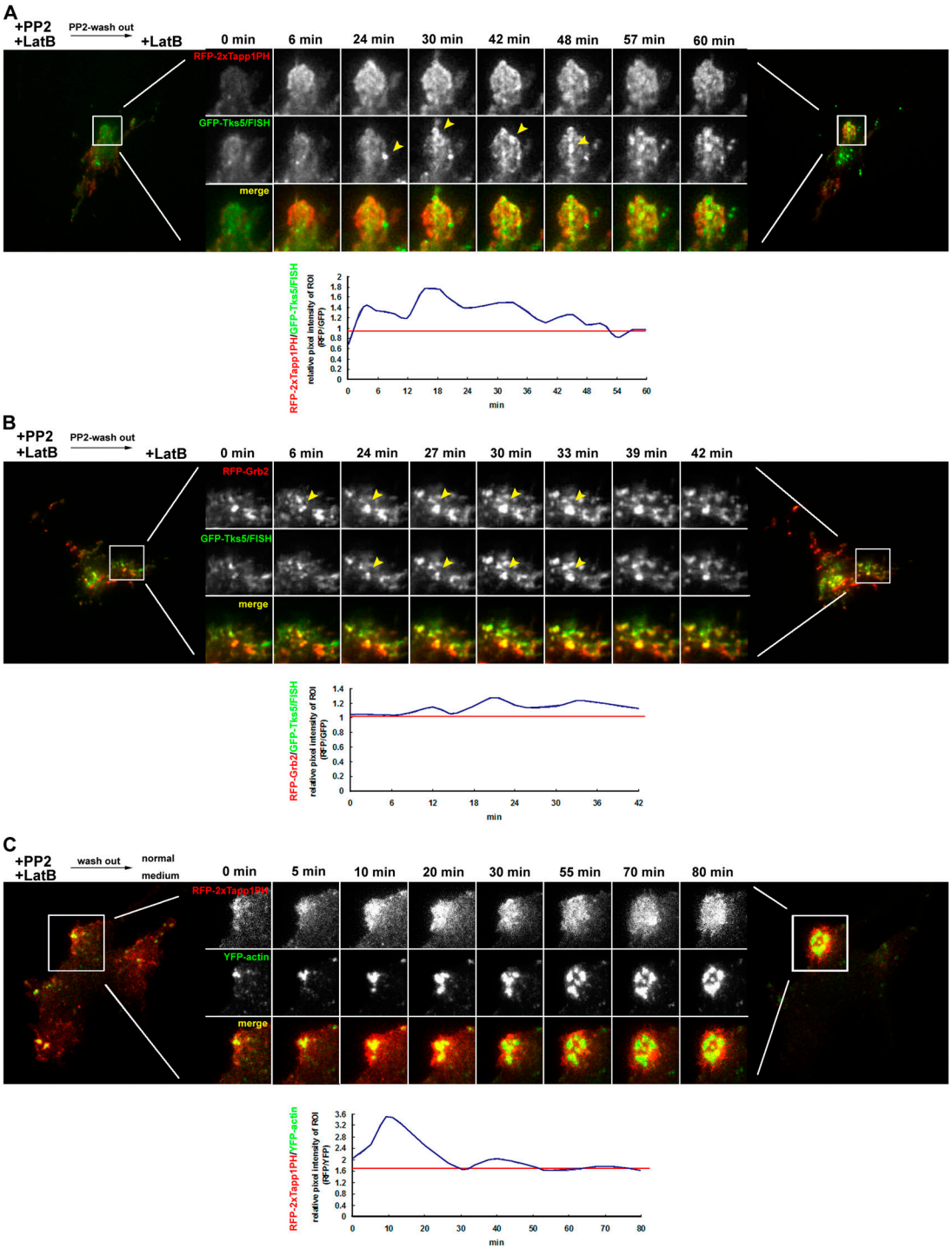

Figure 5. **Live-cell imaging of PtdIns(3,4)P2 generation, Grb2-Tks5/FISH recruitment, and actin polymerization at podosomes.** NIH-src cells expressing RFP-2×Tapp1PH and GFP-Tks5/FISH (A), RFP-Grb2 and GFP-Tks5/FISH (B), or RFP-2×Tapp1PH and YFP-actin (C) were cultured in a fresh medium with (A and B) or without (C) latrunculin B (0.5 μg/ml) after the treatment with PP2 (10 μM) and latrunculin B (0.5 μg/ml) for 30 min. White boxed areas are enlarged to reveal the accumulation of each molecule. Arrowheads indicate Tks5/FISH or Grb2 being recruited to this region. The time that elapsed from the start of the observation is indicated above each column. Representative charts of the relative pixel intensity (RFP/GFP or RFP/YFP) from the enlarged area are also indicated.

full/jcb.200801042/DC1). Interestingly, we observed that ∼5% of NIH-src cells expressing the delta-VCA mutant of N-WASP developed a ring-shaped structure composed of N-WASPΔVCA itself (the remaining 95% localized broadly in the cytoplasm with suppressed podosome formation). This structure possessed phosphorylated Src (at Y416) and FAK at its center (Fig. S5, C and D), colocalized with Tks5/FISH (Fig. S5 E, arrowheads); however, it was devoid of F-actin and cortactin (Fig. S5 F, arrows). This structure is only formed when N-WASPΔVCA expression is moderate in a cell, thus enabling its proper regulation. These data suggest that a podosome precursor comprising Tks5/FISH, Grb2, and N-WASP is formed before actin polymerization

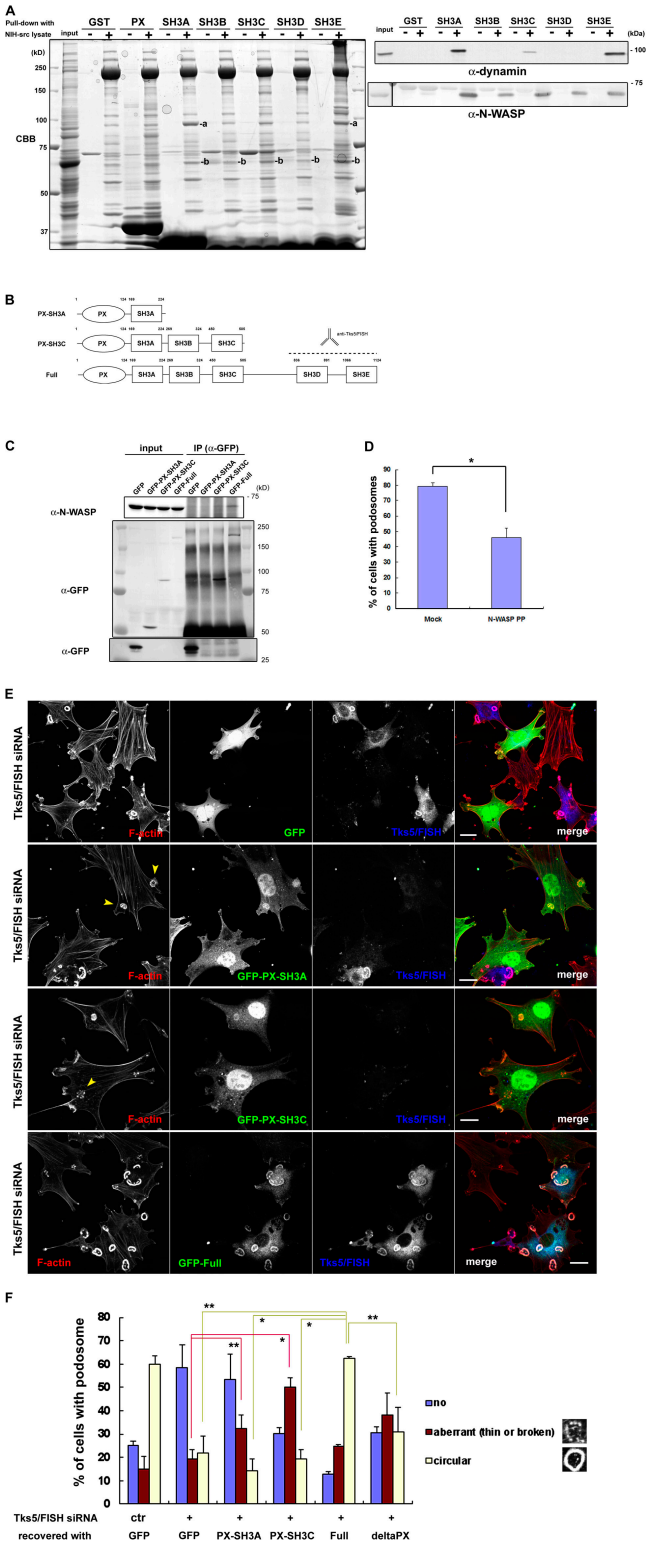

Figure 6. **Tks5/FISH–N-WASP binding promotes podosome formation in NIH-src cells.** (A, left) NIH-src cell lysates were mixed with the GST-PX or GST-SH3 domains of Tks5/FISH immobilized on beads; the bound proteins were resolved by SDS-PAGE, stained with Coomassie Brilliant Blue (CBB), and then subjected to mass spectrometry. (A, right) NIH-src cell lysates were mixed with the GST-SH3 domains of Tks5/FISH immobilized on beads, and the bound proteins were analyzed by using anti-dynamin or anti-N-WASP antibody. (B) Schematic diagrams of the truncated Tks5/FISH constructs used in the assay. Anti-Tks5/FISH antibody (Santa Cruz Biotechnology, Inc.) is raised against amino acid residues expanding SH3D and SH3E of Tks5/FISH. (C) The ability of Tks5/FISH to bind N-WASP depends on its SH3 domains. Cell lysates of NIH3T3 cells expressing GFP-tagged Tks5/FISH constructs were immunoprecipitated by using anti-GFP antibody, and the bound proteins were detected by using anti-N-WASP antibody. The blot of anti-GFP for lower molecular weight was separately shown. (D) The expression of the poly-proline sequence of N-WASP (rat N-WASP, residues 267–390) suppresses podosome formation. *, $P < 0.01$ by Student's *t* test compared with mock-transfected cells. A minimum of 50 cells were counted in each round. Error bars represent standard deviations of three different experiments. (E) GFP-Tks5/FISH constructs rescue podosome formation in NIH-src cells having reduced Tks5/FISH expression. GFP-tagged Tks5/FISH constructs were transfected into NIH-src cells, followed by transfection with Tks5/FISH siRNA. The cells were stained with rhodamine-phalloidin (red) to visualize F-actin and with anti-Tks5/FISH antibody (blue). Arrowheads indicate aberrant podosomes. (F) Cells that exhibited a GFP signal and a weak (Full) or no (GFP, PX-A, PX-C) anti-Tks5/FISH signal were grouped under three categories based on their podosome morphology (no podosomes, aberrant podosomes, or circular podosomes). *, $P < 0.02$; **, $P < 0.05$ by Student's *t* test compared with full length. A minimum of 50 cells were counted in each round. Error bars represent standard deviations of three different experiments. Bars, 20 μm.

and that Tks5/FISH may play a role in arranging N-WASP as a podosome launcher at FAs.

Thus, the molecular mechanisms involved in podosome formation can be summarized as follows: (1) constitutive activation of c-Src accompanied by PtdIns(3)-kinase activation leads to tyrosine phosphorylation of FAK and other FA machineries as well as the generation of PtdIns(3,4)P2 in the vicinity of FAs. (2) Grb2 is targeted to this FA-related adhesion sites (probably through interacting with the phosphorylated site of FAK [Y925]; Mitra et al., 2005) together with Tks5/FISH. Then, the localization of Tks5/FISH at the FA-related adhesion is stabilized via PX-lipid interaction. Simultaneously, dynamin is considered to be recruited to FA-related adhesions via Grb2, and it might help Tks5/FISH recruitment to this site. (3) N-WASP is effectively concentrated near FA-related adhesions by Tks5/FISH, and this leads to intent actin polymerization at these sites (Fig. 7).

Discussion

In this study, we have identified a stepwise mechanism for podosome formation, particularly its initiation. By using phosphoinositide-binding domains, PtdIns(3,4)P2 was shown to be the most concentrated phosphoinositide in podosomes. Further, although Tapp1PH inhibited PtdIns(3,4)P2 signaling, this inhibition was weaker than that of AktPH, which binds both PtdIns(3,4)P2 and PtdIns(3,4,5)P3 (Fig. 1 B). Because the expression of these domains may not be sufficient for blocking phosphoinositides from interacting with downstream targets, it is important to investigate the pathways by which PtdIns(3,4)P2 and PtdIns(3,4,5)P3 are generated. An intriguing aspect would be to investigate the manner in which antecedent PtdIns(3,4)P2 production occurs at adhesion sites in an Src-dependent manner (Fig. 2, A–C; and Fig S2 I). PtdIns(4,5)P2 and type I phosphatidylinositol phosphate kinase isoform-γ, an enzyme that produces PtdIns(4,5)P2, have been suggested to be responsible for the modulation of FAs by their binding to talin and other FA proteins (Di Paolo et al., 2002; Ling et al., 2002, 2006). Likewise, PtdIns(3)-kinase is also known to be activated via the Src-FAK pathway (Hanks

Figure 7. **A model for podosome formation in NIH-src cells.** Tks5/FISH is recruited to FA-related adhesions in a PtdIns(3,4)P2- and Grb2 binding–dependent manner before actin polymerization; this results in N-WASP accumulation near the FA-related adhesions and intense actin polymerization.

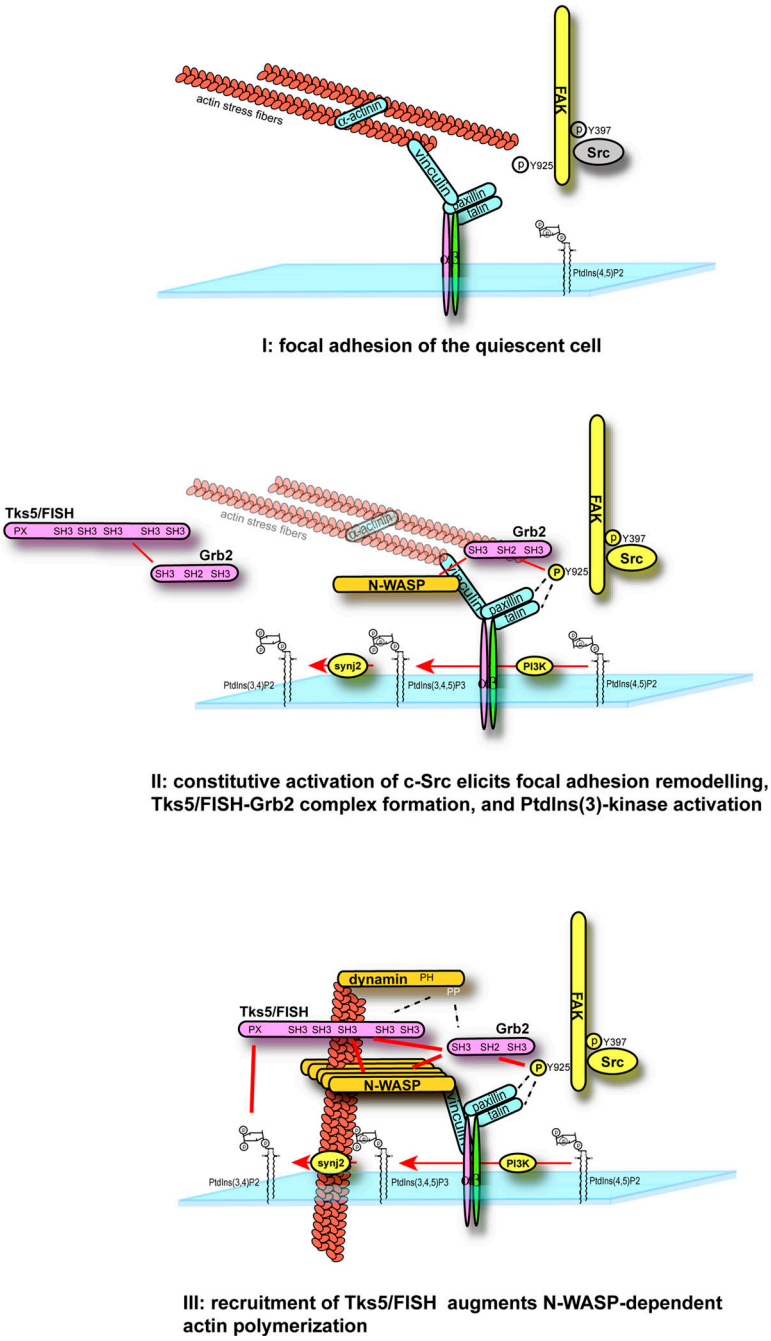

et al., 2003). Therefore, the most likely pathway for PtdIns(3,4)P2 production is via dephosphorylation of PtdIns(3,4,5)P3 by PtdIns(3,4,5)P3 5-phosphatases such as SHIP2, synaptojanin2, and/or SKIP. In fact, synaptojanin2 is inferred to be involved in podosome formation and invasion in NIH-src cells (Fig. S1, D–F) and is reported to play an essential role in invadopodium formation in glioma cells (Chuang et al., 2004). Further, because synaptojanin2 has been identified as a downstream effector for Rac (Malecz et al., 2000) and Rac activity is essential for podosome formation (unpublished data), the hypothesis that the p130Cas-Crk-Rac-synaptojanin2 pathway is involved in PtdIns(3,4)P2 production is plausible (the involvement of Crk is described in Fig. 3 A and Fig. S4 D).

The nature of adhesion sites with PtdIns(3,4)P2 observed in NIH-src cells might be different from that of normal FAs. Live-cell imaging analysis of NIH3T3 cells transfected with active Src revealed that although PtdIns(3,4)P2 production was observed at the proximal of newly formed FAs, it was distinct from FAs themselves (Fig. 2 C). Additionally, vinculin-rings of podosomes were newly assembled at PtdIns(3,4)P2-enriched adhesion sites rather than that preexisting vinculin of FAs were modified into podosomes.

The PX domain of Tks5/FISH has been reported to bind both PtdIns(3)P and PtdIns(3,4)P2 (Abram et al., 2003), and this binding is indispensable for Tks5/FISH localization to podosomes and for Src-dependent podosome formation (Seals

et al., 2005). Given the specific targeting of Tks5/FISH to PtdIns(3,4)P2-enriched FA-related adhesions, the adaptor protein Grb2 is the most likely to help targeting Tks5/FISH at the sites of action because their binding was Src dependent (Fig. 3, B and C). Grb2 is suggested to be involved in podosome formation, whereas another adaptor protein, Nck1, is not (Fig. 3 A). However, a contradictory result was reported: Nck1 but not Grb2 is involved in EGF-induced invadopodium formation in mammary carcinoma cells (Yamaguchi et al., 2005). It is intriguing to speculate that the difference between the integrin-based and growth factor–based triggering mechanisms may explain this discrepancy. In support of this speculation, integrin-mediated invadopodia are not expected to move laterally across the membrane because such movement might be limited by integrin adhesion to a substrate; however, the nascent invadopodia observed by Yamaguchi et al. (2005) are actively motile despite limitations provided to the membrane by a clearly identified moving actin-rich object. Moreover, although the suppressed expression of Nck1 seemed to have little effect on podosome formation itself (Fig. 3 A), significant effect on invasion was observed (Fig. S4 D). Our results suggest that Nck1 would participate in matrix degradation via other mechanisms than podosome formation, where future works should be addressed.

While investigating for proteins that bind to the adaptor molecule Tks5/FISH, we identified dynamin as a binding partner of Tks5/FISH. Dynamin localizes to podosomes in NIH-src cells, and RNAi in dynamin expression suppresses podosome formation (unpublished data), indicating that dynamin plays an essential role in podosome formation. Dynamin has been shown to interact with FAK (probably through Grb2), and it plays a role in microtubule-induced FA disassembly (Ezratty et al., 2005). Thus, it is possible that the FA-related adhesions in NIH-src cells are susceptible to disassembly by the dynamin-FAK system, and this leads to the frequent turnover of podosomes.

We observed that the delta-VCA mutant of N-WASP localizes to form a podosome-like structure and inhibits actin polymerization in NIH-src cells. By using antibodies against several endogenous proteins, Tks5/FISH was found to colocalize with rings of N-WASPΔVCA, whereas cortactin was absent (Fig. S5, E and F). Recently, live-cell imaging analysis of Src-transformed breast carcinoma cells has revealed that actin–cortactin aggregates in invadopodia support the subsequent accumulation of membrane type 1 matrix metalloproteinase (MT1-MMP) in invadopodia, which is required for the initiation and sustenance of matrix degradation (Artym et al., 2006). Therefore, these ring-shaped aggregates that contain Tks5/FISH and N-WASP but not cortactin could be considered as podosome precursors, and the formation of these would be followed by actin polymerization and matrix degradation involving cortactin. Further, we observed that these podosome precursors are formed around FA-related adhesions (Fig. S5, C and D), implying that the precursors interact with the FA-related adhesions and/or the plasma membrane surrounding them.

In conclusion, based on the results of RNAi, protein interaction, and live-cell imaging analysis, we have established a stepwise mechanism for podosome formation (Fig. 7). Podosomes initiate from FAs due to changes in the phosphorylation status of proteins and in the composition of phosphoinositides on the plasma membrane. The onset of actin polymerization is triggered by Tks5/FISH recruitment and subsequent N-WASP accumulation. This step involves intricate interactions of Tks5/FISH with both phosphoinositides and Grb2.

Materials and methods

Reagents and antibodies

The following antibodies were used: rabbit anti-Tks5/FISH, anti-Grb2, anti-synaptojanin2, and monoclonal mouse anti-myc (Santa Cruz Biotechnology, Inc.); monoclonal mouse anti-FAK, monoclonal mouse anti-Grb2, and anti-dynamin (BD Biosciences); rabbit anti-Nck, monoclonal mouse anti-c-Src, and anti-cortactin (Millipore); rabbit anti-c-Src, anti-phospho-Src, anti-Crk, anti-myc, and monoclonal mouse anti-HA (Cell Signaling Technology); monoclonal mouse anti-vinculin and anti-γ-tubulin (Sigma-Aldrich); rabbit anti-GFP (MBL International); and rabbit anti-N-WASP. Latrunculin B and LY294002 were purchased from Sigma-Aldrich. PP2 was purchased from BIOMOL International, L.P.

Plasmid construction and mutagenesis

All Tks5/FISH constructs were generated by polymerase chain reaction (PCR) using mouse cDNA as the template, and their identity was confirmed by sequencing. The 2,600th nucleotide of the Tks5/FISH cDNA was observed to be adenine in three different cDNA libraries (BD Biosciences), although it is registered as thymine in a database (GenBank/EMBL/DDBJ accession no. AJ007012). This mutation results in a V867G-point mutation. To produce GST-tagged PX and SH3 domains of Tks5/FISH, the cDNA was cloned into pFASTBAC and pGEX6P-1 (GE Healthcare), respectively. To generate GFP and RFP fusion proteins, cDNA encoding full-length and truncated regions of Tks5/FISH or Grb2 was cloned into pEGFP C-1 (Clontech Laboratories, Inc.) and pTagRFP-C (Evrogen). Further, cDNA of the lipid-binding domains (Furutani et al., 2006) and the PX domains of Tks5/FISH were cloned into pCMV3B (Stratagene), pCMVHA, or pTagRFP-C. Site-specific mutagenesis was performed by PCR using mutated primers.

Generation of stable NIH3T3 cell lines

NIH3T3 cells were transfected with pcDNA or pcDNA-SrcY530F, encoding a mutant form of human Src encompassing an activating Y530F substitution, with Lipofectamine 2000 (Invitrogen). Single colonies were isolated after 2–3 wk of G418 selection (1.0 mg/ml). Protein expression was assessed by immunoblotting of cell lysates with anti-phospho-Src antibody. The resultant cells were termed as NIH-ctr or NIH-src.

Cell culture and transfection

NIH3T3, NIH-ctr, and NIH-src cells were cultured at 37°C in DME containing 10% calf serum (CS) and penicillin/streptomycin under 5% CO_2. To obtain transient expression, the cells were plated at 40% confluence on a 6-well plate, and on the following day they were incubated with 1.6 μg DNA and 3.5 μl Lipofectamine 2000 (Invitrogen) in Opti-MEM (Invitrogen) for 6 h. After this, they were transferred to a complete medium and cultured for 18 h. The cells were then replated onto type 1-C collagen (Nitta Gelatin)-coated coverslips and cultured for an additional 24 h before analysis. For siRNA transfection, the cells were plated at 20% confluence on a 6-well plate, and on the following day they were incubated with 160 pmol siRNA and 4.0 μl Lipofectamine 2000 (Invitrogen) or 6.0 μl RNAi MAX (Invitrogen) in Opti-MEM (Invitrogen) for 6 h. They were then cultured in a complete medium for 18 h before a second round of siRNA transfection. The cells were then replated and analyzed as described above. To prevent PtdIns(3)-kinase activity, the cells were treated with 25 μM LY294002 for 40 min before fixation. To prevent Src-kinase activity, the cells were treated with 10 μM PP2 for 40 min before fixation.

Matrigel invasion assay

The NIH-src cells (2.0×10^4 cells) were plated on a BioCoat Matrigel Invasion Chamber (BD Biosciences) for 18 h with DMSO, PP2, or LY294002. For transfection analysis, two rounds of siRNA or DNA transfection was performed 48/72 h before plating on the chamber. After this, the chambers were fixed in 3.7% formaldehyde in PBS for over 30 min. The chambers were then washed in PBS, and the invaded cells were stained with crystal violet. After washing the cells with PBS more than three times, cells from three different sample points on the lower surface of the chamber were counted.

RNAi experiments

The following stealth siRNA (Invitrogen) derived from mouse *N-WASP*, *Tks5/FISH*, *Nck1*, *Grb2*, *Crk*, or *synaptojanin2* cDNA, respectively, were used for the RNAi experiments: siRNA for N-WASP (5′-AUAGUCACACAUUUCUUGCCGAGGA-3′ or 5′-AAGCGACACCACUGCACUUCUUUGC-3′), Tks5/FISH (5′-UUGCCUGGAAGAAAGGGAAUAAUCC-3′ or 5′-AAGCUGAUCUCUUUCUUGGUGAUGG-3′), Nck1 (5′-UAUCAAUGACAACUCAUCCUCUCUC-3′ or 5′-UAUUUAGGUUAUUGACAACUGCUGC-3′), Grb2 (5′-AAUAUCUGCUGGUUCCUGGACACGG-3′ or 5′-AGAAUUAAACUUCACCACCCACAGG-3′), Crk (5′-CAAUGUUGUAGUGUCCAAAUAGUGU-3′ or 5′-AUUAAUCUUCGUAACCUUUACCAGC-3′), and synaptojanin2 (5′-AUUGGGCCAUGCGAAAUAGAACACC-3′ or 5′-UUAUUCCAGUUCUAGCCUUGGGUGG-3′). The control siRNA sequences were designed by scrambling one of the targeted oligos of each molecule. Silencing of WAVE1 and WAVE2 by RNAi was performed with the pSUPER vector constructs described previously (Kurisu et al., 2005). In the rescue experiment, GFP-Tks5/FISH constructs were transfected 24 h after replating, as described in the previous section.

Immunofluorescence

The cells cultured on type 1-C collagen-coated coverslips were fixed in 3.7% formaldehyde in PBS or 2% paraformaldehyde in PBS. They were permeabilized with 0.1% Triton X-100 in PBS for 5 min and then incubated with primary antibodies for over 60 min. They were then washed with PBS and incubated with secondary antibodies and rhodamine-phalloidin (Invitrogen) for 30 min. Finally, the cells were washed with PBS and mounted on glass slides.

Live-cell imaging of NIH-src cells

NIH-src cells transfected with the indicated constructs were grown on type 1-C collagen-coated glass-base dishes (IWAKI). After treatment with PP2 (10 µM) and latrunculin B (0.5 µg/ml), the medium was replaced with new medium with or without latrunculin B (0.5 µg/ml). The images were acquired for 30–80 min at 3- or 5-min intervals by using a TIRF microscopy system.

Image acquisition and processing

All photographic images of cells were taken through Eclipse E600 (Nikon), Axiovert 200M (Carl Zeiss, Inc.), IX 81 (Olympus), or IX71 (Olympus) microscopes with respective confocal microscopy or TIRF systems (Radiance 2000 [Bio-Rad Laboratories], LSM510META [Carl Zeiss, Inc.], FV1000 [Olympus], or ION LASER [MELLES GRIOT] equipped with a Cascade II cooled charge-coupled devise [CCD] camera [Photometrics]) at RT, except the image acquired in Fig. 2 C at 37°C. 40× objective, NA 0.90 (Olympus), 60× oil immersion objective, NA 1.35 (Olympus), 60× oil immersion objective, NA 1.40 (Nikon), 63× oil immersion objective, NA 1.4 (Carl Zeiss, Inc.), or 100× oil immersion objective, NA 1.45 (Olympus) were used. Fluorochromes used include AlexaFluor 488, 546, 647, and rhodamine-labeled phalloidin (all Invitrogen). Gels or blots were scanned with a scanner (model GT-X900; Epson). Images were assembled with Photoshop (Adobe). In each plate, photographs were cropped and each fluorochrome was adjusted identically for brightness and contrast to represent the observed images.

Mass spectrometry

The NIH-src cell lysates (10 mg) were pulled down with GST-tagged Tks5/FISH constructs conjugated to glutathione sepharose 4B (GE Healthcare). The proteins bound to the constructs were resolved by one-dimensional SDS-PAGE and visualized by using Coomassie Brilliant Blue (CBB). The bands of interest were excised from the gel by using acetonitrile containing 5% formic acid and 0.1% trifluoroacetic acid. The peptides were purified by liquid chromatography and analyzed by matrix-assisted laser desorption/ionization time-of-flight mass spectrometry/mass spectrometry (MALDI/TOF-MS/MS; 4700 Proteomics Analyzer; Applied Biosystems). The detected masses and peptides sequences were subjected to database searches using the Mascot search engine (Matrix Science).

Immunoprecipitation

The NIH-ctr or NIH-src cells treated with DMSO or PP2 (10 µM) for 40 min were washed with cold PBS and lysed with RIPA lysis buffer (50 mM Tris, pH 7.5, 150 mM NaCl, 1 mM EDTA, 1% TritonX-100, 1% sodium deoxycholate, and 0.1% SDS) supplemented with 2 µg/ml aprotinin, 2 µg/ml leupeptin, 1 mM PMSF, and 1 mM sodium orthovanadate. The cell lysates were pre-cleared with preimmune rabbit IgG (Santa Cruz Biotechnology, Inc.) with immobilized protein A (Thermo Fisher Scientific); subsequently, Grb2 or Tks5/FISH was immunoprecipitated with anti-Grb2 (rabbit polyclonal) or anti-Tks5/FISH antibody, respectively.

Protein expression and purification

The His-GST-tagged PX domain of the Tks5/FISH proteins was expressed in Sf9 cells and purified on glutathione-sepharose beads (GE Healthcare) according to a standard method. The GST-tagged SH3 domains of Tks5/FISH, Grb2, and the SH2 domain of Grb2 were expressed in *Escherichia coli* and bound to glutathione-sepharose beads for the pull-down assay.

Statistics

Statistically significant differences were determined using the Student's *t* test. Differences were considered significant if $P < 0.05$.

Online supplemental material

Fig. S1 shows the involvement of Src, PtdIns(3)-kinase, and synaptojanin2 in podosome formation and invasion activity of NIH-src cells. Fig. S2 shows the importance of the PX domain of Tks5/FISH in targeting PtdIns(3,4)P2 on the plasma membrane. Fig. S3 shows the assembly of podosomes at the proximal of newly formed adhesions. Fig. S4 shows the involvement of Nck1, Grb2, or Crk in podosome formation and invasion activity of NIH-src cells. Fig. S5 shows the involvement of N-WASP in podosome formation and invasion activity of NIH-src cells. Online supplemental material is available at http://www.jcb.org/cgi/content/full/jcb.200801042/DC1.

We are grateful to Dr. S. Kurisu for the pSuper constructs.

T. Takenawa was supported by a Grant-in-Aid for Cancer from the Ministry of Education, Culture, Sports, Science, and Technology of Japan. T. Oikawa was supported in part by the Takeda Science Foundation.

Submitted: 8 January 2008
Accepted: 11 June 2008

References

Abram, C.L., D.F. Seals, I. Pass, D. Salinsky, L. Maurer, T.M. Roth, and S.A. Courtneidge. 2003. The adaptor protein fish associates with members of the ADAMs family and localizes to podosomes of Src-transformed cells. *J. Biol. Chem.* 278:16844–16851.

Alvarez, R.H., H.M. Kantarjian, and J.E. Cortes. 2006. The role of Src in solid and hematologic malignancies: development of new-generation Src inhibitors. *Cancer.* 107:1918–1929.

Artym, V.V., Y. Zhang, F. Seillier-Moiseiwitsch, K.M. Yamada, and S.C. Mueller. 2006. Dynamic interactions of cortactin and membrane type 1 matrix metalloproteinase at invadopodia: defining the stages of invadopodia formation and function. *Cancer Res.* 66:3034–3043.

Buccione, R., J.D. Orth, and M.A. McNiven. 2004. Foot and mouth: podosomes, invadopodia and circular dorsal ruffles. *Nat. Rev. Mol. Cell Biol.* 5:647–657.

Carman, C.V., P.T. Sage, T.E. Sciuto, M.A. de la Fuente, R.S. Geha, H.D. Ochs, H.F. Dvorak, A.M. Dvorak, and T.A. Springer. 2007. Transcellular diapedesis is initiated by invasive podosomes. *Immunity.* 26:784–797.

Chellaiah, M.A. 2006. Regulation of podosomes by integrin alphavbeta3 and Rho GTPase-facilitated phosphoinositide signaling. *Eur. J. Cell Biol.* 85:311–317.

Chuang, Y.Y., N.L. Tran, N. Rusk, M. Nakada, M.E. Berens, and M. Symons. 2004. Role of synaptojanin 2 in glioma cell migration and invasion. *Cancer Res.* 64:8271–8275.

Co, C., D.T. Wong, S. Gierke, V. Chang, and J. Taunton. 2007. Mechanism of actin network attachment to moving membranes: barbed end capture by N-WASP WH2 domains. *Cell.* 128:901–913.

David-Pfeuty, T., and S.J. Singer. 1980. Altered distributions of the cytoskeletal proteins vinculin and alpha-actinin in cultured fibroblasts transformed by Rous sarcoma virus. *Proc. Natl. Acad. Sci. USA.* 77:6687–6691.

Destaing, O., F. Saltel, J.C. Geminard, P. Jurdic, and F. Bard. 2003. Podosomes display actin turnover and dynamic self-organization in osteoclasts expressing actin-green fluorescent protein. *Mol. Biol. Cell.* 14:407–416.

Di Paolo, G., L. Pellegrini, K. Letinic, G. Cestra, R. Zoncu, S. Voronov, S. Chang, J. Guo, M.R. Wenk, and P. De Camilli. 2002. Recruitment and regulation of phosphatidylinositol phosphate kinase type 1 gamma by the FERM domain of talin. *Nature.* 420:85–89.

Ezratty, E.J., M.A. Partridge, and G.G. Gundersen. 2005. Microtubule-induced focal adhesion disassembly is mediated by dynamin and focal adhesion kinase. *Nat. Cell Biol.* 7:581–590.

Furutani, M., K. Tsujita, T. Itoh, T. Ijuin, and T. Takenawa. 2006. Application of phosphoinositide-binding domains for the detection and quantification of specific phosphoinositides. *Anal. Biochem.* 355:8–18.

Gimona, M. 2008. The microfilament system in the formation of invasive adhesions. *Semin. Cancer Biol.* 18:23–34.

Hanks, S.K., L. Ryzhova, N.Y. Shin, and J. Brabek. 2003. Focal adhesion kinase signaling activities and their implications in the control of cell survival and motility. *Front. Biosci.* 8:d982–d996.

Itoh, T., and T. Takenawa. 2004. Regulation of endocytosis by phosphatidylinositol 4,5-bisphosphate and ENTH proteins. *Curr. Top. Microbiol. Immunol.* 282:31–47.

Jurdic, P., F. Saltel, A. Chabadel, and O. Destaing. 2006. Podosome and sealing zone: specificity of the osteoclast model. *Eur. J. Cell Biol.* 85:195–202.

Kurisu, S., S. Suetsugu, D. Yamazaki, H. Yamaguchi, and T. Takenawa. 2005. Rac-WAVE2 signaling is involved in the invasive and metastatic phenotypes of murine melanoma cells. *Oncogene.* 24:1309–1319.

Linder, S., D. Nelson, M. Weiss, and M. Aepfelbacher. 1999. Wiskott-Aldrich syndrome protein regulates podosomes in primary human macrophages. *Proc. Natl. Acad. Sci. USA.* 96:9648–9653.

Linder, S., H. Higgs, K. Hufner, K. Schwarz, U. Pannicke, and M. Aepfelbacher. 2000. The polarization defect of Wiskott-Aldrich syndrome macrophages is linked to dislocalization of the Arp2/3 complex. *J. Immunol.* 165:221–225.

Ling, K., R.L. Doughman, A.J. Firestone, M.W. Bunce, and R.A. Anderson. 2002. Type I gamma phosphatidylinositol phosphate kinase targets and regulates focal adhesions. *Nature.* 420:89–93.

Ling, K., N.J. Schill, M.P. Wagoner, Y. Sun, and R.A. Anderson. 2006. Movin' on up: the role of PtdIns(4,5)P(2) in cell migration. *Trends Cell Biol.* 16:276–284.

Lock, P., C.L. Abram, T. Gibson, and S.A. Courtneidge. 1998. A new method for isolating tyrosine kinase substrates used to identify fish, an SH3 and PX domain-containing protein, and Src substrate. *EMBO J.* 17:4346–4357.

Malecz, N., P.C. McCabe, C. Spaargaren, R. Qiu, Y. Chuang, and M. Symons. 2000. Synaptojanin 2, a novel Rac1 effector that regulates clathrin-mediated endocytosis. *Curr. Biol.* 10:1383–1386.

Marchisio, P.C., L. Bergui, G.C. Corbascio, O. Cremona, N. D'Urso, M. Schena, L. Tesio, and F. Caligaris-Cappio. 1988. Vinculin, talin, and integrins are localized at specific adhesion sites of malignant B lymphocytes. *Blood.* 72:830–833.

Mitra, S.K., D.A. Hanson, and D.D. Schlaepfer. 2005. Focal adhesion kinase: in command and control of cell motility. *Nat. Rev. Mol. Cell Biol.* 6:56–68.

Mizutani, K., H. Miki, H. He, H. Maruta, and T. Takenawa. 2002. Essential role of neural Wiskott-Aldrich syndrome protein in podosome formation and degradation of extracellular matrix in src-transformed fibroblasts. *Cancer Res.* 62:669–674.

Olivier, A., L. Jeanson-Leh, G. Bouma, D. Compagno, J. Blondeau, K. Seye, S. Charrier, S. Burns, A.J. Thrasher, O. Danos, et al. 2006. A partial down-regulation of WASP is sufficient to inhibit podosome formation in dendritic cells. *Mol. Ther.* 13:729–737.

Seals, D.F., E.F. Azucena Jr., I. Pass, L. Tesfay, R. Gordon, M. Woodrow, J.H. Resau, and S.A. Courtneidge. 2005. The adaptor protein Tks5/Fish is required for podosome formation and function, and for the protease-driven invasion of cancer cells. *Cancer Cell.* 7:155–165.

Soriano, P., C. Montgomery, R. Geske, and A. Bradley. 1991. Targeted disruption of the c-src proto-oncogene leads to osteopetrosis in mice. *Cell.* 64:693–702.

Takenawa, T., and T. Itoh. 2001. Phosphoinositides, key molecules for regulation of actin cytoskeletal organization and membrane traffic from the plasma membrane. *Biochim. Biophys. Acta.* 1533:190–206.

Takenawa, T., and T. Itoh. 2006. Membrane targeting and remodeling through phosphoinositide-binding domains. *IUBMB Life.* 58:296–303.

Tarone, G., D. Cirillo, F.G. Giancotti, P.M. Comoglio, and P.C. Marchisio. 1985. Rous sarcoma virus-transformed fibroblasts adhere primarily at discrete protrusions of the ventral membrane called podosomes. *Exp. Cell Res.* 159:141–157.

Yamaguchi, H., M. Lorenz, S. Kempiak, C. Sarmiento, S. Coniglio, M. Symons, J. Segall, R. Eddy, H. Miki, T. Takenawa, and J. Condeelis. 2005. Molecular mechanisms of invadopodium formation: the role of the N-WASP-Arp2/3 complex pathway and cofilin. *J. Cell Biol.* 168:441–452.

Yamaguchi, H., F. Pixley, and J. Condeelis. 2006. Invadopodia and podosomes in tumor invasion. *Eur. J. Cell Biol.* 85:213–218.

Yeatman, T.J. 2004. A renaissance for SRC. *Nat. Rev. Cancer.* 4:470–480.